

An analysis of double exposure lithography options

Saul Lee^a, Jeffrey Byers^b, Kane Jen^a, Paul Zimmerman^b, Bryan Rice^b, Nicholas J. Turro^c, and C. Grant Willson^a

^aDepartment of Chemical Engineering, The University of Texas at Austin, Austin, Texas, USA;

^bSEMATECH, 2706 Montopolis Drive, Austin, Texas, USA;

^cDepartment of Chemistry, Columbia University, New York, New York, USA

ABSTRACT

The current optical photolithography technology is approaching the physical barrier to the minimum achievable feature size. To produce smaller devices, new resolution enhancement technologies must be developed. Double exposure lithography has shown promise as potential pathway that is attractive because it is much cheaper than double patterning lithography and it can be deployed on existing imaging tools. However, this technology is not possible without the development of new materials with nonlinear response to exposure dose. The performance of existing materials such as reversible contrast enhancement layers (rCELS) and theoretical materials such as intermediate state two-photon (ISTP) and optical threshold layer (OTL) materials in double exposure applications was investigated through computer simulation. All three materials yielded process windows in double exposure mode. OTL materials showed the largest process window (DOF 0.137 μm , EL 5.06 %). ISTP materials had the next largest process window (DOF 0.124 μm , EL 3.22 %) followed by the rCEL (0.105 μm , 0.58 %). This study is an analysis of the feasibility of using the materials in double exposure mode.

Keywords: Double Exposure Lithography, Immersion Lithography, Double Patterning Lithography, Resolution Enhancement Techniques

1. INTRODUCTION

The current technological progression of the photolithography industry has reached a limit in the maximum achievable resolution. Resolution as determined by the half pitch critical dimension (CD) is limited by the Rayleigh equation

$$CD = \frac{k_1 \cdot \lambda}{NA}, \quad (1)$$

where k_1 is the process aggressiveness factor, λ is the wavelength of the imaging tool, and NA is the numerical aperture of the imaging lens. To reduce the half pitch CD , the industry must reduce k_1 or λ , or increase NA . The theoretical minimum value for k_1 with single exposure is 0.25, but the generally accepted manufacturability limit is 0.27. The current industry standard imaging tool has a wavelength of 193 nm. Future imaging tools are proposed to operate in the Extreme Ultra Violet (EUV) range with a λ of 13.4 nm, however, the EUV technology will most likely not be viable until after 2013. With water immersion lithography, the maximum achievable NA is approximately 1.35. Increasing the NA requires simultaneous development of a high index lens material along with high index fluids and high index resists. Without major breakthroughs in optical materials, NA will plateau near 1.35. Given these parameters, the current CD limit is approximately 38 nm half pitch.

To enable lithography at sub 38nm half pitch, the industry will need to consider alternative resolution enhancement technologies. Two exposure passes have been proposed as a possible resolution enhancement technique for existing photolithography imaging systems. A single mask with high feature density that is difficult to resolve can be split into two exposures each with lower feature density that can be easily resolved. When combined, the two exposures replicate the original mask.

Further author information: Send correspondence to Professor C. Grant Willson

Mail: 1 University Station C0400, Austin, TX, 78712

E-mail: willson@che.utexas.edu

1.1 Double Exposure Lithography versus Double Patterning Lithography

Double exposure lithography (DEL) and double patterning lithography (DPL) are proposed approaches to performing the two exposure passes. DEL is defined as a two exposure pass lithographic process that does not require the removal of the wafer from the exposure tool chuck between passes. DPL is defined as a two exposure pass lithographic process that requires a chemical development of the photoresist layers and possibly an intermediate etch step. The DPL processing approaches will require the removal of the wafer from the exposure tool chuck and loss of overlay registration. DEL and DPL processes are illustrated in Figure 1. The benefits of

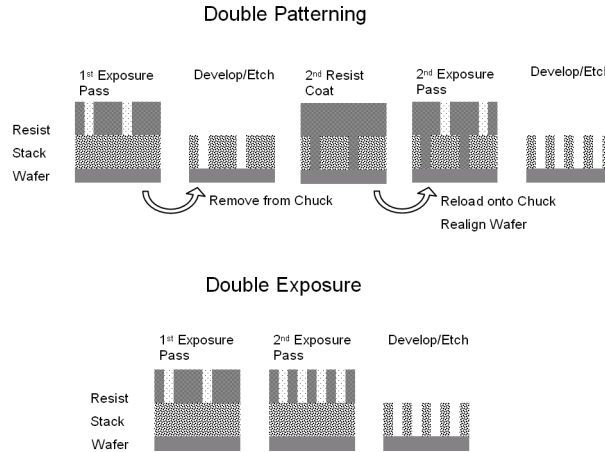


Figure 1. Comparison of the double patterning lithography(development/etch scheming shown) and double exposure lithography processes.

DEL and DPL principally include the ability to use existing exposure tools to print technology nodes below the NA limit for single exposure processes. This could mean a lower cost of ownership as these techniques can in principle be deployed without costly capital investment. However, the two exposure passes require doubling the number of masks and reduced throughput due to increased processing time. The process time is dramatically increased in the DPL process because of the additional process steps compared to the DEL process. In addition, the removal of the wafer from the wafer chuck between exposures poses severe overlay issues that may be difficult to overcome, especially at the CDs where this technology will be implemented. The DEL process only introduces an additional exposure pass, and since the wafer is not removed from the imaging tool between exposures, the overlay issues are minimized. The reduced cost of ownership of DEL suggests that it would be the preferred technique.

1.2 “Resist Memory” Effect

The DEL infrastructure is currently available on existing state of the art exposure tools. However, imaging below a k_1 value of 0.25 with double exposure is impossible without the development of new materials. Conventional resists have a “memory” effect that prevents proper replication of the mask image. That is, sub-threshold exposure in the first exposure pass reduces the dose required to render the resist soluble in the second exposure pass. For example, the normalized aerial image intensities for the first exposure pass reaching the resist of equal lines and spaces can be described by the following

$$I_{pass1} = A \cos^2 \frac{\pi \cdot X}{pitch} + B, \quad (2)$$

where A is a constant describing the amplitude and B is the minimum image intensity. For the second exposure pass, the mask and, consequently, the aerial image are translated by half pitch and lead to the following intensity function

$$I_{pass2} = A \cos^2 \frac{\pi \cdot X}{pitch} + \frac{\pi}{2} + B = A \sin^2 \frac{\pi \cdot X}{pitch} + B. \quad (3)$$

The photochemical response of the resist results in a linear summation of the absorbed intensities from the two exposure pass. This leads to the following intensity function within the resist

$$I_{Sum} = I_{Pass1} + I_{Pass2} = A \cos^2 \frac{\pi \cdot X}{pitch} + A \sin^2 \frac{\pi \cdot X}{pitch} + 2B = A + 2B = \text{a Constant!} \quad (4)$$

Consequently, the two individual mask images are not resolved when double exposed. This concept is illustrated in Figure 2.

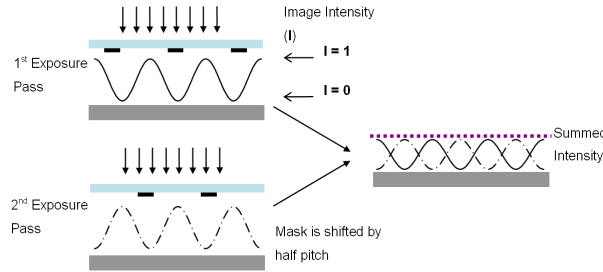


Figure 2. Summation of the intensity of two exposure passes and the effect of dose reciprocity.

The resist system converts the separate light images, intensity versus position, into chemical images, chemical composition versus position. Mathematically, this conversion of the light image into a chemical image can be represented by a translation function $f(I)$. In the case of standard resist systems, this translation function has the linear addition property

$$f(I_{Pass1} + I_{Pass2}) = f(I_{Pass1}) + f(I_{Pass2}). \quad (5)$$

Resolving the mask features requires a material with a nonlinear response to exposure such that

$$f(I_{Pass1} + I_{Pass2}) = f(I_{Pass1}) + f(I_{Pass2}) \quad (6)$$

and the “resist memory” behavior is minimized.

1.3 Potential DEL Materials

Several materials have been proposed to implement a nonlinear response to exposure and theoretically permit double exposure pitch doubling including contrast enhancement layers (CELs), two-photon materials, intermediate state two-photon (ISTP) materials, and optical threshold layers (OTLs). These materials and their theory of operation are described in the following sections.

1.3.1 Contrast Enhancement Layer

Contrast enhancement layers (CELs) are strongly absorbing materials that increase transparency, or photobleach,¹ when exposed to light. A CEL is normally applied directly on top of the resist layer. During exposure, energy is first devoted to photobleaching the CEL. As the CEL becomes transparent, the energy is then able to reach the resist and initiate the solubility switch. Light can only penetrate through the CEL in regions where aerial image intensities are high (non-opaque regions on the mask) and cannot reach the resist in regions where aerial image intensities are lower (opaque regions on the mask). This introduces a nonlinear transfer of the applied aerial image into the photoresist and improves the resolution. CELs can be divided into two different subtypes, namely, reversible (rCEL) and irreversible (irCEL). The main difference between the two subtypes is that, in rCELs, the photobleached regions can return to the initial opaque state between exposure passes whereas in irCELs, the photobleaching is irreversible. Details on the existing chemistries and transmission characteristics for CELs have been described in previously published work²⁻⁶ and are not discussed here.

1.3.2 Two-Photon Materials

Two-photon photoresist systems involve the incorporation of photoacid generators (PAGs) that require the simultaneous absorption of two photons to induce the photochemical acid generation. The chemical reaction for a two-photon photoacid generator can be described by the following reaction



where σ is the quantum efficiency of the two-photon photochemical reaction. Since the simultaneous absorption of two photons is required for the reaction, the probability of conversion is proportional to the light intensity squared, which provides a nonlinear response to exposure energy

$$f(I) \approx I \cdot I \quad (8)$$

and the DEL conversion is

$$f(I_{PASS1}) + f(I_{PASS2}) \approx I_{PASS1} \cdot I_{PASS1} + I_{PASS2} \cdot I_{PASS2} = f(I_{PASS1} + I_{PASS2}). \quad (9)$$

Unlike the CEL, two-photon materials are not enhancement layers that are applied on top of existing resists, but rather the nonlinear response is incorporated directly into the resist formulation. This eliminates complexities introduced by the addition of an extra film layer such as depth of focus and material compatibility.

Two-photon resist systems for microfabrication using laser writing systems have been reported previously.⁷ These systems employ specially designed PAGs with high two-photon absorbance cross sections. High efficiency two-photon PAGs have not yet been developed to work with 193 nm. Analysis (to be presented in future work) of the two-photon reaction kinetics suggests that a very large increase in exposure source output would be required to produce a viable level of process throughput. As such, the two-photon material type was not included in the simulation studies.

1.3.3 Intermediate State Two-Photon Materials

Intermediate state two-photon (ISTP) layers are materials that generate acid molecules in a reversible two step process. Similar to two-photon materials, ISTP materials alter the acid generation behavior of the resist medium. Although each step requires the absorption of a photon, ISTP materials are not true two-photon processes in that the acid production does not have a quadratic dependence on dose. The reaction sequence is



where σ_1 and σ_2 represent the cross-sections and τ_1 and τ_2 represent the lifetimes of the species.

Although ISTP materials do not exhibit true two-photon behavior, they may require significantly lower doses to generate acid compared to two-photon resists. The trade off between lower reaction orders may be offset by the lower doses. The behavior of ISTP materials depends on the ability of the intermediate species to revert to the initial state. A build up of the intermediate species will effectively render the sequence to become a first ordered reaction that is controlled by a rate limiting step. Therefore, the characteristics of the exposing laser such as the energy per pulse (A_0), pulse cycle time (t_f , also the inverse of the repetition rate), and full width half max (FWHM) also have to be considered.

1.3.4 Optical Threshold Materials

Optical threshold layers (OTLs) are materials that require the absorption of a threshold exposure dose to induce a photochemical event. The exposure threshold gives the material a region of nonlinear response to exposure dose and allows OTLs to be used as double exposure resists. Nonlinearity derives from the fact that any dose absorbed below the threshold does not cause reactions to occur.

Above the dose threshold, a step change in conversion occurs and is described by the following piecewise function

$$f(I) = \begin{cases} [PAC]_{th} & , E_{Actual} \geq E_{th} \\ 1 & , E_{Actual} < E_{th} \end{cases} , \text{ where } E_{Actual} = \frac{I \cdot dt}{\text{pulses}} \quad (11)$$

where E_{Actual} and E_{th} represent the actual dose received by the material and the threshold dose, respectively. $[PAC]_{th}$ is the step wise conversion concentration of the photoactive compound after reaching E_{th} . Equation 11 shows the behavior of an ideal OTL material.

Analogous thermal resist systems are already in use in the printing industry.⁸ Thermal resists rely upon a thermal image instead of an optical image. These systems can, for example, function by exploitation of a phase change that is inherently threshold-like. If a material is heated to a temperature just below its melting point and then cooled, it does not “remember” the previously applied thermal dose. Chapman et al. have investigated inorganic thermal resist systems⁹ that use Bi/In bilayers as an etch masking layer for silicon. However, the use of Bi and In metals are not compatible with the photolithography process as the target semiconductor devices are very susceptible to metal contamination. Chemical systems with similar properties for optical images have to be developed to use this technology with lithographic imaging systems.

1.4 Feasibility Studies

These materials are not the only possibilities, but they do provide a reasonable range of resist designs to explore the feasibility of DEL as a technology choice. Of the proposed materials, only CELs and two-photon materials have been extensively studied and have established chemical systems. ISTP and OTL materials do not currently exist for use in semiconductor applications. However, their theoretical mechanisms are considered to test their viability as a possible DEL candidates. This work investigates the feasibility of the materials for use in DEL applications through simulation and is meant to guide our materials development effort.

2. SIMULATION CONDITIONS

The performance of the different material types in double exposure mode and the dependence on their material properties were evaluated by computer simulation using a combination of PROLITH lithography simulator and custom code. In all cases, the optical imaging portion was performed with PROLITH. The material responses of the reversible CEL was studied using the PROLITH simulator. However, commercial models for the ISTP and OTL materials do not yet exist as the materials are not currently used in production, so a custom simulator was developed to model the material behaviors in these systems.

2.1 Imaging Setup

A half pitch CD of 25 nm was targeted using a 1.2 NA water immersion exposure system in double exposure mode. This is an effective k_1 of 0.155. An azimuthally polarized cross-quadrupole with $center = 0.8$ and $radius = 0.15$ was used as the illuminator. Different masks were used for each of the two exposure passes. The masks were 50 nm line/space phase shift masks with 6 % attenuation. The two masks were offset by 50 nm between exposure passes. As described previously,² DEL with positive tone resists is a trench-based process as opposed to the line-based process expected with a single exposure pass. Consequently, the target line is expected to form at the interface of the opaque and bright regions as opposed to the center of the bright regions. A focus-exposure matrix was run for each material system, and the resulting CD was observed.

Table 1. Parameters used for the base resist system.

Property	Value
n	1.70
Dill A (μm^{-1})	0
Dill B (μm^{-1})	1.47
Dill C (cm^2/mJ)	0.0478
[Q]/[PAG]	0.2
M_{th}	0.75
D_H (nm^2/s)	0.223
D_Q (nm^2/s)	0.0
k_a (1/s)	0.100
k_b (1/s)	4.85×10^8

2.2 Film Stack and Base Resist System

The film stack consisted of 50 nm of resist on 31 nm of a single layer of bottom anti-reflective coating (BARC) ($n = 1.82$, $k = 0.46$). The substrate was silicon with a 2 nm layer of SiO_2 . The resist simulations were based upon a typical 193 nm resist system. The base resist parameters are shown in Table 1. In the case of the OTL and ISTP materials, the acid generation behavior differs from the base resist and was described with custom models.

2.3 Reversible CEL Simulation Parameters

To study the CEL behavior, a 50 nm CEL was applied on top of the film stack. The Dill A parameter was varied from $10 \mu\text{m}^{-1}$ to $50 \mu\text{m}^{-1}$. The CEL parameters are shown in Table 2. Since a reversible CEL system provides

Table 2. Simulation parameters used for the reversible CEL material.

Parameter	Value
n	1.69
Dill A μm^{-1}	0 - 50
Dill B μm^{-1}	0
Dill C (cm^2/mJ)	0.11

better performance than an irreversible system, the rCEL was selected for the study.

2.4 ISTP Simulation Parameters

To study the performance of the ISTP material, the acid generation behavior described in the previous section was solved using a 4th order Runge-Kutta method.¹⁰ The parameters and values used in the simulation are listed in Table 3. To simplify the calculations, γ_2 was assumed to be very large such that the conversion of the intermediate species to acid is assumed to be irreversible.

2.5 OTL Simulation Parameters

The OTL acid generation behavior described in the previous section was implemented. A dose threshold, E_{th} , of $10 \text{ mJ}/\text{cm}^2$ was used with a threshold photoacid compound conversion, $[PAC]_{th}$, value of 0.75.

Table 3. Simulation parameters used for the ISTP material.

Parameter	Value
γ_1 (cm ² /mJ)	0.235
γ_2 (cm ² /mJ)	0.235
t_1 (s)	0.006
t_f (s)	0.00025
A_0 (mJ/cm ²)	0.05
	1
FWHM (ns)	20

3. RESULTS AND DISCUSSION

All three materials yielded nonlinear resist response when used in double exposure mode. The resist profiles are shown in Figure 3 to Figure 5 and summarized in Table 4.

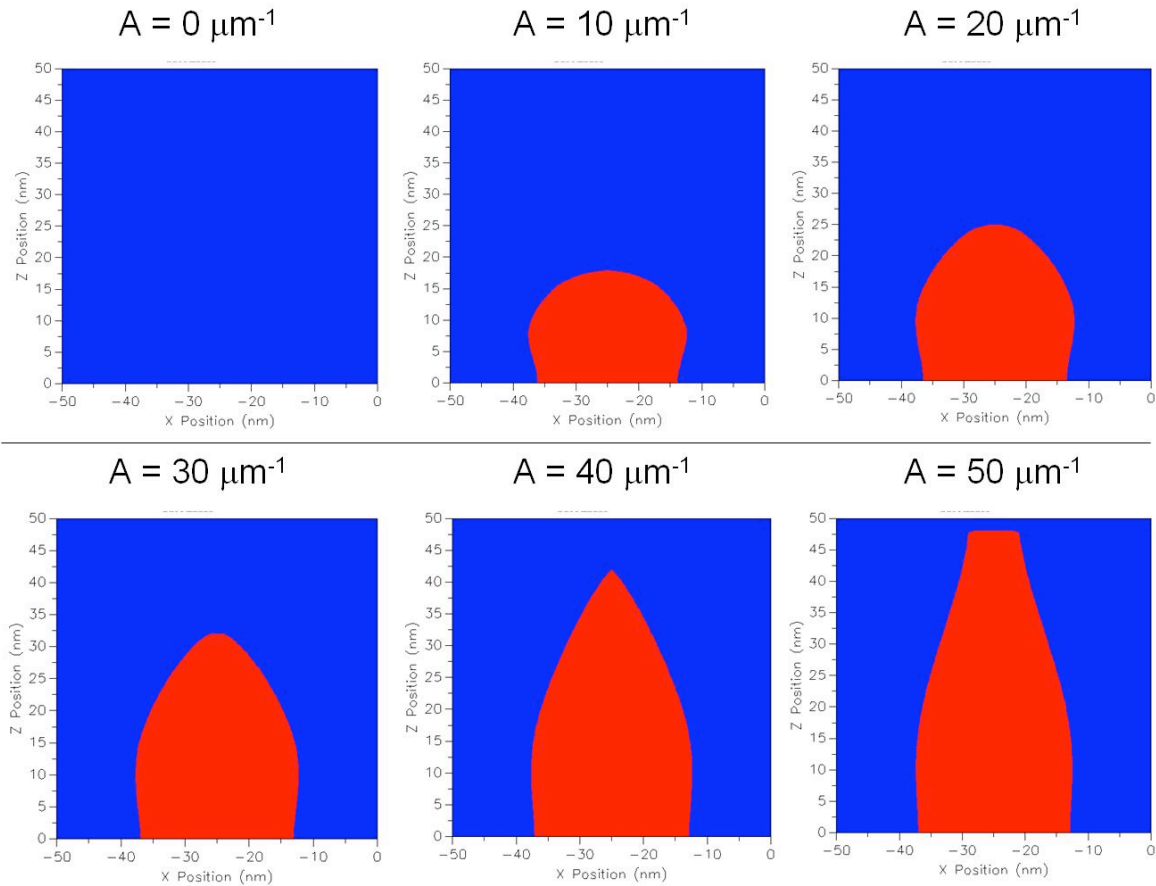


Figure 3. Resist profile of rCEL with varying Dill A parameter.

The simulation results from the focus-exposure experiments were analyzed using ProDATA to generate simulated Bossung plots and exposure latitude (EL) versus depth of focus (DOF) plots. The results are shown in

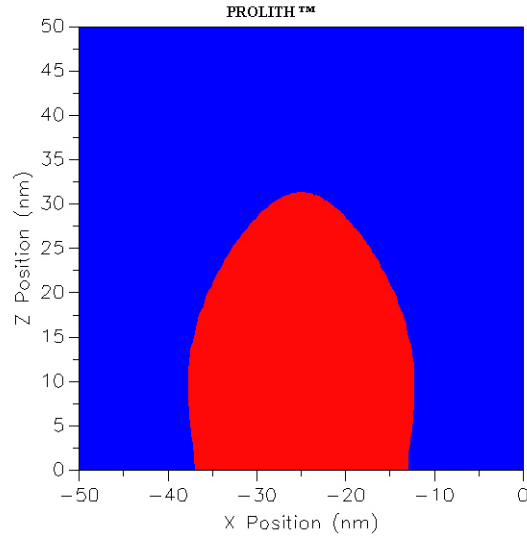


Figure 4. Resist Profile for ISTP material.

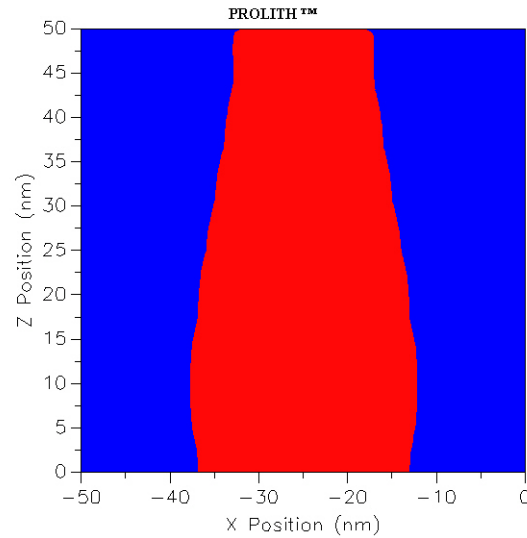


Figure 5. Resist Profile for OTL material.

Figure 6 to Figure 8 and are summarized in Table 5. Simulated EL versus DOF plots with respect to the different Dill A parameters are shown in Figure 9.

It is important to note that CD was the only output metric considered in the process window calculations. In most manufacturing environments, other parameters such as sidewall angle and resist loss would also need to be optimized to produce functional devices. However, the main goal of this work is to demonstrate the proof of concept of the theoretical materials. Optimization of such parameters is beyond the scope of this work.

Figure 3 shows the effects of the Dill A parameter on the resist profile. For the test case of a Dill A parameter of $0 \mu\text{m}^{-1}$, no resist profile was observed. This finding is consistent with the behavior of conventional resists since no nonlinearity was applied and further verified that the DEL process does not provide resolved images in conventional resists.

In all cases, increasing the Dill A parameter decreased resist loss and improved the shape of the resulting image. Figure 9 shows that the process window was also widened with the increase. Increasing the Dill A param-

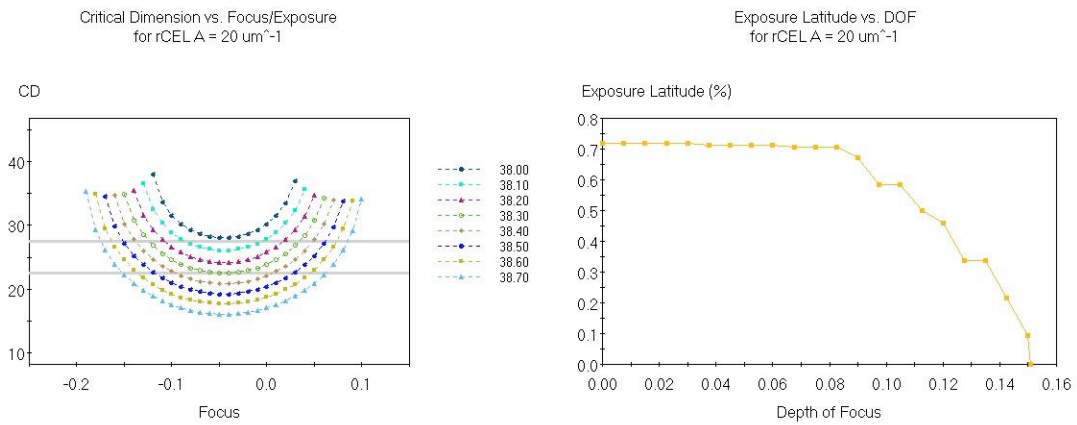


Figure 6. Simulated Bossung plot and EL versus DOF for rCEL material.

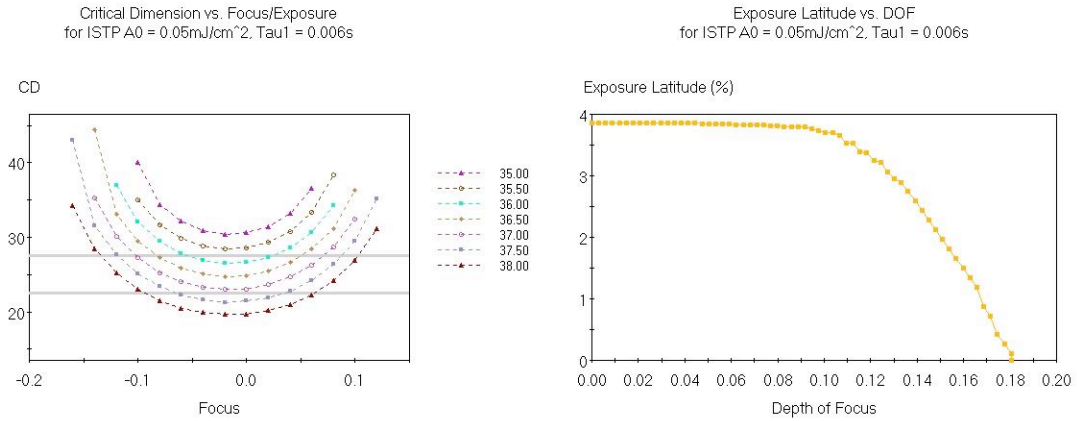


Figure 7. Simulated Bossung plot and EL versus DOF for ISTP material.

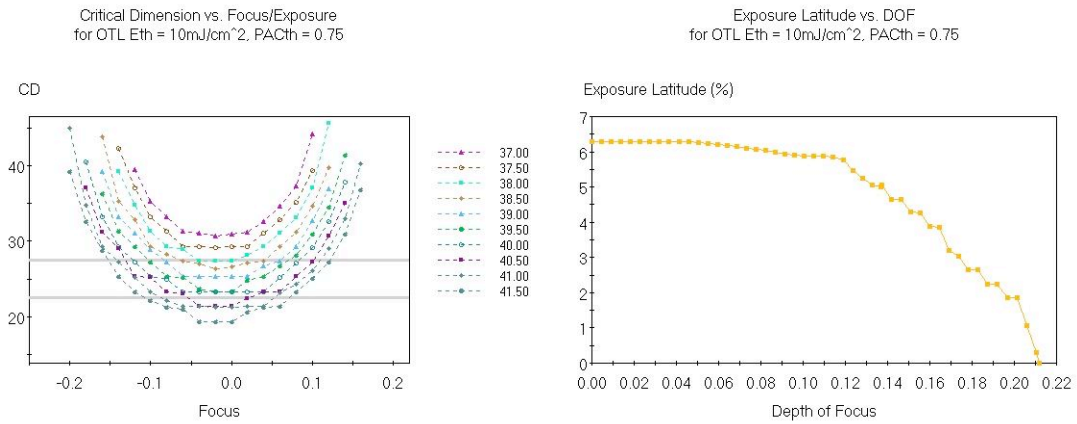


Figure 8. Simulated Bossung plot and EL versus DOF for OTL material.

Table 4. Summary of resist profile metrology.

Material	Dose (mJ/cm ²)	Sidewall Angle (°)	Resist Loss (nm)
rCEL A = 10 μm^{-1}	24.6	74.9	32.2
rCEL A = 20 μm^{-1}	38.2	74.4	25.0
rCEL A = 30 μm^{-1}	56.4	71.1	18.0
rCEL A = 40 μm^{-1}	79.6	70.2	8.1
rCEL A = 50 μm^{-1}	108	74.8	2.0
ISTP	36.5	71.9	18.8
OTL	39.3	81.9	0.2

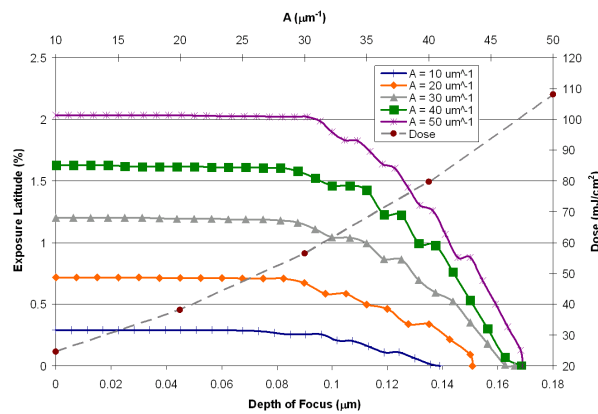


Figure 9. Process windows of rCEL materials varying the Dill A parameter.

eter showed improvement for EL. However, only marginal improvement was observed for the DOF. Increasing the Dill A parameter also led to increases in the dose requirement. An increase in the Dill A parameter from 10 μm^{-1} to 50 μm^{-1} required approximately 4.4 fold increase in dose. Another factor to consider is the feasibility of obtaining rCEL materials with high Dill A values. Without increasing the Dill A parameter, it is theoretically possible to increase the absorbance of the rCEL layer by increasing the layer thickness. However, the oblique incident angles resulting from operating at NA values greater than 1 may lead to loss in depth of focus if the layer becomes too thick. rCEL materials showed nonlinear behavior in DEL mode, however, image quality and process window improvement was only observed for rCELs with very high Dill A parameters ($> 30 \mu\text{m}^{-1}$). Even if physical analogs with such high Dill A parameters are obtainable, the improvements are marginal and come at the cost of large dose increases.

Table 4 shows that an rCEL with Dill A parameter of 20 μm^{-1} has a comparable dose requirement to that of ISTP and OTL materials. Results from this run were used for subsequent comparisons with ISTP and OTL materials.

Figure 4 shows the resist profile of the ISTP material. The profile is comparable to rCEL having slightly lower sidewall angle, 71.9°, and reduced resist loss, 18.8 nm. Table 5 shows that ISTP has a larger process window than rCEL. The parameters of interest affecting the nonlinear acid generation behavior of the material are the energy delivered per pulse, A_0 , and the reversible rate constant of the intermediate state, $1/\tau_1$. For a given set of laser parameters, large values of A_0 or $1/\tau_1$ lead to faster conversion of PAC thus reducing the required exposure dose. However, the dose reduction also leads to a decrease in nonlinearity. Since the laser can only deliver integer numbers of pulses, the magnitude of A_0 has to be within a manageable increment such that small

Table 5. Summary of process windows for the rCEL, ISTP, and OTL materials.

Material	Depth of Focus (μm)	Exposure Latitude (%)
rCEL	0.105	0.58
ISTP	0.124	3.22
OTL	0.137	5.06

deviations in the pulse delivery will not drastically affect the CD. The parameters had to be optimized so that the system will retain nonlinear behavior but at the same time yield features within reasonable exposure dose ranges. ISTP materials showed a larger process window and improved resist profile than rCEL, and could be a potential DEL material provided that materials with the specified kinetics and time constants can be identified.

Figure 5 shows the resist profile of the OTL material. The profile shows a significant reduction in resist loss compared to both rCEL and ISTP resist profiles and slight improvement in the sidewall angle. The OTL material also has the largest process window of the three materials investigated. The threshold dose requirement behavior of the OTL material served effectively to filter out regions of low intensity. In addition, the threshold conversion response of the PAC resulted in improved image contrast. Because no such physical systems exist, the threshold dose, E_{th} , and PAC conversion, $[PAC]_{th}$, were chosen such that they would provide a defined solubility switch within comparable dose ranges. Performance in physical systems may differ depending on the thresholding mechanism. OTL materials showed the best performance (i.e. largest process window and best resist profile) compared to rCEL and ISTP materials and would be suitable for DEL applications. This suggests that potential mechanisms, either chemical or physical, need to be explored.

4. CONCLUSIONS

DEL offers several advantages over DPL, but it requires new materials with nonlinear dose response. We have employed simulations to explore several potential DEL material options. The modeling results show that two-photon materials will not be feasible unless achievable laser peak power in exposure tools can be significantly increased. rCEL materials demonstrated nonlinear behavior in DEL mode, however, image quality and process window improvement was only observed for rCELs with very high Dill A parameters ($> 30 \mu\text{m}^{-1}$). Even if physical analogs with such high Dill A parameters are obtainable, the improvements are marginal. ISTP materials showed a larger process window than rCEL. The challenges with this approach are identifying materials with the specified kinetics and the ability to tune the time constants. OTL materials showed the best performance with the largest process window and best resist profile. There are no physically functional optical analogs with the thresholding behavior. Potential mechanisms, either chemical or physical, need to be explored. From our feasibility studies, we believe that the ISTP and OTL materials have the greatest potential for use in DEL applications and warrant our investment in materials development.

ACKNOWLEDGMENTS

The authors would like to thank SEMATECH for financial support of this project, KLA-Tencor for the donations of PROLITH and ProDATA licenses, Mark Smith and Trey Graves of KLA-Tencor, and Intel Corporation for the donations of simulation machines.

Disclaimers

SEMATECH, and the SEMATECH logo are registered servicemarks of SEMATECH, Inc. All other servicemarks and trademarks are the property of their respective owners.

REFERENCES

- [1] Gri ng, B. F. and West, P. R., "Contrast enhanced lithography," *Solid State Technology* 28(5), 152–7 (1985).
- [2] Byers, J., Lee, S., Jen, K., Zimmerman, P., Turro, N. J., and Willson, C. G., "Double exposure materials: Simulation study of feasibility," *Journal of Photopolymer Science and Technology* 20(5), 707–717 (2007).
- [3] Krayushkin, M. M., Uzhinov, B. M., Martynkin, A. Y., Dzhavadov, D. L., Kalik, M. A., Ivanov, V. L., Stoyanovich, F. M., Uzhinova, L. D., and Zolotarskaya, O. Y., "Thermally irreversible photochromic dithienylethenes," *International Journal of Photoenergy* 1(3), 183–190 (1999).
- [4] Becker, R. S. and Michl, J., "Photochromism of synthetic and naturally occurring 2H-chromenes and 2H-pyrans," *Journal of the American Chemical Society* 88(24), 5931–3 (1966).
- [5] Grant, B. D., Clecak, N. J., Twieg, R. J., and Willson, C. G., "Deep UV photoresists I. Meldrum's diazo sensitizer," *IEEE Transactions on Electron Devices* 28(11), 1300–1305 (1981).
- [6] West, P. R., Davis, G. C., and Gri ng, B. F., "Contrast enhanced photolithography: application of photo-bleaching processes in microlithography," *Journal of Imaging Science* 30(2), 65–8 (1986).
- [7] Kuebler, S. M., Braun, K. L., Zhou, W., Cammack, J. K., Yu, T., Ober, C. K., Marder, S. R., and Perry, J. W., "Design and application of high-sensitivity two-photon initiators for three-dimensional microfabrication," *Journal of Photochemistry and Photobiology A: Chemistry* 158(2-3), 163–170 (2003).
- [8] Gelbart, D. and Karasyuk, V. A., "UV thermoresists: sub-100-nm imaging without proximity effects," *Proc. SPIE* 3676(2), 786–793 (1999).
- [9] Chapman, G. H., Tu, Y., and Peng, J., "Wavelength invariant Bi/In thermal resist as a Si anisotropic etch masking layer and direct-write photomask material," *Proc. SPIE* 5039, 472–483 (2003).
- [10] Chapra, S. C. and Canale, R. P., [*Numerical Methods For Engineers: With Software and Programming*], McGraw-Hill, New York, 4th ed. (2002).